An Industrial Perspective on Catalysts for Low temperature CO_2 Electrolysis

Richard I. Masel[1]*, Zengcai Liu[1], Hongzhou Yang[1], Jerry J. Kaczur[1], Daniel Carillo[1], Shaoxuan Ren[2], Danielle Salvatore[2], Curtis P. Berlinguette[2]

[1]Dioxide Materials, 3998 FAU Blvd #300, Boca Raton Fl, USA

[2]Department of Chemistry, University of British Columbia, 2036 Main Mall, Vancouver, BC Canada V6T 1Z1

Abstract

Electrochemical conversion of CO_2 to useful products at temperatures below 100 °C are nearing the commercial scale. Pilot units for CO_2 conversion to CO are already in testing. Units to convert CO_2 to formic acid are projected to reach pilot scale in the next year. Further, several investigators are starting to observe industrially relevant rates of the electrochemical conversion of CO_2 conversion to ethanol and ethylene with the needed hydrogen coming from water. In each case, Faradaic efficiencies of 80% or more and currents above 200 mA/cm² can be reproducibly achieved.

In this paper we describe the key advances in nano catalysts that lead to the impressive performance, indicate where additional work is needed and provide benchmarks that others can use to compare their results.

Main

The conversion of CO_2 via electrolysis is a growing field. In 2019, there were over 600 papers describing catalyst improvements. There have been many recent reviews[5,37-42]. The growth of the field is being driven by three main influences: i) the falling price of renewable energy, ii) the need to decarbonize the economy, and iii) that the processes are starting to become commercially relevant.

This paper will focus on a few key developments in the field with an emphasis on advances from 2018-2020. Major advances from 2018 to the present include:

- Electrolyzers for the conversion of CO_2 into CO are reaching pilot scale[1-6].
- One can now directly form formic acid from CO_2 and not a formate[6-10].
- Production of C_2 products is now beginning to show industrially significant rates[11-17].
- Two-step electrolysis, where CO is produced in one electrolyzer, and converted in a second electrolyzer is now showing renewed interest[18-23].
- Supported organometallic[24], MOF[25,26] and single atom catalysts[27,28] are starting to show promising rates.
- Ligands to direct surface reactions playing a key role in improving selectivity[29-36].

We do not include a review of the findings from theory. Christensen et al.[43] found that conventional density functional calculations have systematic errors when applied to CO_2 conversion, with activation energy changes as large as 50 kJ/mol with small changes in the functional[44,45]. Also, we have been asked to limit the number of papers we cite, so there were many wonderful papers that could not be included in this review.

Electrochemical Conversion of CO_2 to CO

We will start by describing the electrochemical conversion of CO_2 to CO, since this application is closest to commercialization. Dioxide Materials[4,6], Opus 12 and Siemens[1-3] are each developing pilot scale low temperature electrolyzers. Smaller systems are being developed at other companies. (High temperature systems being developed by Haldor Topsoe are not featured here.) Generally, one feeds humidified CO_2 to the cathode of an electrolyzer and circulates water with some electrolyte into the anode as indicated in Figure 1. CO_2 reacts with water on the cathode via the reaction:

$$CO_2 + H_2O + 2\ e^- \rightarrow CO + 2OH^-$$

the OH^- crosses through the membrane to the anode where it reacts via the reaction

$$2OH^- \rightarrow H_2O + \tfrac{1}{2}\ O_2 + 2\ e^-$$

The net reaction is:

$$CO_2 \rightarrow CO + \tfrac{1}{2}\ O_2$$

At one point there were issues with catalyst stability, but at this point stable long-term performance has been achieved. The catalyst stability is highly related to the cell configuration and the testing conditions. For example, Haas et al. [3] reported that cell voltage varied by 0.5 V during 1200 hr run at 300 mA/cm^2 and 30 °C with catholyte flowing between cathode and diaphragm membrane. Liu et al. [46] found that they could run a CO_2 electrolyzer at 200 mA/cm² for 3800 hours at room temperature using zero-gap cell configuration. The voltage needed to maintain a current density of 200 mA/cm² increased by only 11 mV in 3800 hours (~3µ V/hr). The average Faradaic efficiency for CO formation averaged 97% during this run. The equilibrium voltage for CO formation is 1.44 V. One is able to detect onset of CO formation at an applied voltage of 1.5 V, but the currents are tiny. The CO current reaches about 10 mA/cm² at a cell potential of 2.0 V and then rises exponentially as the voltage is increased. The current per unit area reaches 100 mA/cm² at about 2.6 V and 500 mA/cm² at 3-3.1 V. Stable on-off performance has also been achieved.[5] Higher currents are possible. For example, currents of ~0.5 A/cm² have been demonstrated in pilot scale electrolyzers running at 50 °C[5]. That corresponds to a current of 250 A/gm of silver. Edwards et al.[47], report a strikingly high 1.5 A/cm² at similar voltages by pressuring the electrolyzer to 50 bar, circulating KOH through the anode. Clearly industrially relevant currents are possible for CO_2 electrolysis to CO.

Table 1 Industrial benchmarks for electrolyzers to convert CO_2 to CO

Electrolyzer current	200-500 mA/cm²
Catalyst activity	>100 A/gm
Faradaic Efficiency	>95%
Voltage increase at constant current	<10 µV/hr
Turnovers demonstrated	>70,000,000[5]
Turnovers target	>500,000,000

Table 1 shows some other industrial benchmarks for electrolyzer performance. Currents between 200 and 500 mA/cm² and greater than 95% faradaic efficiency are routine. Higher currents can be obtained but industrial CO_2 electrolyzers are difficult to operate at currents above 500 mA/cm² due to overheating in the stack and issues with water management at the higher voltages required. We do not know lifetimes yet because experiments that run long enough to show failures have not yet been done. But the voltage rise at constant current is a measure of system life. A voltage rise of 10 µV/hr suggests a system life between 2 and 3 years. A voltage rise of 3µ V/hr implies a lifetime of about 7 years.

Keys to meeting the benchmark performance include:

- Mounting the cathode catalyst in a gas diffusion layer[48-50] with appropriate ionomers to create a three-phase interface between the CO_2 gas, the catalyst and the ionomer. This strategy reduces mass transfer limitations to obtain high currents.

- Using a zero-gap design[6,51-53] with the anode and cathode catalysts pushed against a highly conductive polymer. This eliminates the ionic resistance, and thereby lowers the cell voltage. Dioxide Materials uses their own Sustainion® anion exchange membranes[54-56]. Siemens uses a PFSA (i.e. PEM) membrane that has been coated with anionic ionomer[57,58].
- Circulating a dilute electrolyte through the anode to keep the membrane hydrated and the cell cooled. Dioxide Materials circulates a 0.01 M $KHCO_3$ solution. KOH solutions have also been used[47,59], but the KOH solutions absorb CO_2, so they are not useful in commercial CO_2 electrolyzers.
- Optimizing the particle size. Years ago, Salehi-Khojin et al.[60,61] showed that the activity of a CO_2 catalyst is the highest if the particle size is 5-10 nm. This work was expanded by Kim et al. [62] and Zhang et al.[63]. The optimum particle size seems to be about 5 nm for silver[60-62] although any silver particles in the range of 5-20 nm show similar activity. Gold particles have an optimum of about 8 nm[64] although gold nanowires have a smaller optimum diameter[65] and there is some contradictory data[66]. Presently, commercial silver nanoparticles with a size between 5 nm and 20 nm is optimum.
- Controlling the humidity in the CO_2 feed to prevent flooding[67] in the cathode catalyst layer and membrane dehydration.
- Running the experiments for thousands of hours to accurately measure catalyst stability.

Many other procedures have been used in the literature as summarized in the supplemental material. Still, one can maximize the industrial relevance of ones' work by:

- Mounting the catalyst on a gas diffusion layer
- Testing in a zero-gap cell
- Reporting the actual cell voltage, not an IR corrected voltage
- Measuring and reporting the voltage increase at constant current - preferably at a current >200 mA/cm²

At this point there have been many valiant efforts to improve silver catalysts for the conversion of CO_2 to CO by changing the catalyst morphology or adding alloying elements as reviewed elsewhere[68,69]. Structures include porous films[70], and hollow spheres[71]. Ag/Cu[72-75], Ag/Zn,[76] Ag/Pd[77,78] and Ag/In alloys[79,80] have also been tried. Unfortunately, most of the newly developed silver catalysts have not approached the 250 A/gm with 95%+ faradaic efficiency and thousand+ hour stability seen with commercially available silver nanoparticle catalysts. There are two exceptions. Recently, Abeyweera et al.[81] reported that porous Ag nanostructures showed currents of 500 A/gm. A coral structure also shows high activity[82]. Further work is needed to determine whether these catalysts are stable enough to be useful industrially.

In contrast, gold catalysts have the potential of exceeding the performance of silver catalysts in several commercial applications such as those where impurities are present in the CO_2 feed. So far, the published work has only used pure CO_2. Early efforts by Jhong et al. [83] Verma et al.[84] and Zhu et al.[64] showed currents in the order of 500 A/gm of gold, albeit at modest selectivity. Improvements have been made to enable selectivities over 90% on gold nanoparticles[85-89] or nanowires[65,90]. These are commercially relevant currents and selectivities.

As with silver, there have been many attempts to improve gold catalysts for CO_2 electrolysis. Changes in morphology have been considered[91,92], but the resulting catalysts showed modest activity on a per gold atom basis. Alloying with silver had modest effects[93,94]. At this point no one has reported tests of gold catalysts under conditions where one might expect gold to be advantageous (e.g., impure CO_2 streams), so it is unclear whether gold nanoparticle catalysts will be superior to silver under any conditions given that gold is 50-70 times more expensive than silver at current 2020 market pricing. Clearly, more work is needed.

Many other metals have been tested for CO_2 conversion to CO. Copper-indium core-shell structures show reasonable currents[95] but lifetime still needs to be demonstrated. Other copper alloys show lower activity[96]. Other metals have been tried but so far none of the other metals or alloys show the combination of activity and stability that is needed for industrial applications of CO_2 conversion to CO.

The next question is whether likely improvements in the cathode catalyst activity will have a significant effect on the economics of the industrial process. Figure 2A shows how the projected cost of producing CO varies with the applied voltage. Generally, the cost of the process is largely determined by three factors: the cost of electricity, the cost of periodic membrane electrode assembly (MEA) replacement, and the cost of the balance of plant (BOP). Notice that the cost to replace the MEA drops substantially as one increases the cell voltage from 2 to 3 V while the electricity cost increases more slowly. The rapid drop in the cost to replace the MEA occurs because the cell current increases from 10 mA/cm^2 to 380 mA/cm^2 as one raises the voltage from 2 to 3 V. Consequently, one needs a much smaller MEA, less expensive, at 3 V than at 2 V to produce the same amount of product.

Figure 2A shows that there is a minimum in the curve at 3.0 V. The minimum occurs when the decrease in the cost of MEA replacement with increasing voltage balances the increase in the cost of electricity with increasing voltage.

Now consider the effect of a 200 mV reduction in the overpotential for CO formation. The current at 3 V doubles but the optimum voltage drops from 3.0 V to 2.8 V so the optimum current is still about 400 mA/cm^2. There is a reduction in the electricity cost of (3.0-2.8)/3.0 = 6.7%. In such a case, one could pay \$0.053/kWh rather than \$0.050/kWh for electricity and still have an economic process assuming that the catalyst lifetime does not decrease. But that is not significant industrially. Instead, one would need to reduce the overpotential by at least 500 mV to have a significant effect on the process economics.

Reductions in the catalyst lifetime can be significant though. Most industrial users will not buy an electrolyzer whose MEA needs to be replaced every year. Further, a reduction in the time between membrane replacement from five years to one year raises the cost by 15%.

One might also ask how the cost of the cathode catalyst affects the economics. Figure 2B shows the breakdown of the cost of the MEA. Notice that cost of the silver catalyst is only 3.7% of the cost of the MEA.

Next we will discuss immobilized molecular catalysts and single atom catalyst (SAC) for electrochemical CO_2 conversion to CO. Molecular CO_2RR catalysts are discrete complexes with well-defined structure. The ligand about the metal can be designed to control the electron density of the reactive metal site, steric effects, and the secondary coordination sphere.[97] Such platforms are therefore particularly valuable for studying specific details of reaction mechanisms. A major challenge in studying homogeneous molecular CO_2RR catalysts is that they tend not to survive a high number of catalytic turnovers. Notwithstanding, the lifetimes of these catalysts can be extended by fixing them to a solid support.

The method of immobilization and the support material has a large effect on catalytic performance[98-100]. Strategies for immobilizing molecular catalysts include utilizing non-covalent interactions of porous conductive surfaces, polymer encapsulation, covalently grafting, and integration into metal organic frameworks (MOFs) or covalent organic frameworks (COFs). Solid supports that have been tested include graphene[101], carbon nanotubes[102], carbon cloth[103], carbon black[104], and nanowires[105]. To illustrate the positive effects of immobilizing a catalyst, consider that a homogeneous cobalt phthalocyanine catalyst yields a FE for CO production of 13% at 0.062 mA/cm^2 for a turnover number of 4[106]. Immobilizing this same catalyst to carbon nanotubes increases the FE to 90% at 10 mA/cm^2 [107]. This reaction enhancement arises from the high surface area and high conductivity of the support, along with the close proximity of the catalyst to the support, providing more efficient delivery of electrons to each catalyst and to more catalysts. This configuration also reduces aggregation and bypasses undesired side reactions to suppress catalyst deactivation[104].

Other means of immobilizing molecular catalysts include the use of polymer encapsulation[108]. This technique can also enhance CO_2RR activity by modifying the coordination spheres and controlling for proton inventory; e.g., the turnover frequency for CoPc was improved from 0.6 s^{-1} to 4.8 s^{-1} upon encapsulation in poly(4-vinylpyridine) (P4VP). The means by which the polymer binds to the metal can also affect the CO_2RR reaction pathways[109]. Incorporating molecular building blocks in porous reticular frameworks presents the opportunity to create discrete active sites with acute control of the surrounding chemical environment[110,111]. The current density of these frameworks can be enhanced by supporting with carbon black and using more conductive linkages[112]. Two dimensional porphyrin based COF materials are also of particular interest due to the facilitated charge carrier mobility by intralayer π-conjugation and interlayer π-π stacking[113-115].

Covalent grafting also enhances catalyst stability. This technique provides for a stronger interaction with the surface than the van der Waals forces used for physisorbed systems. Covalent grafting can be done chemically[116,117] or electrochemically[118,119]. Grafting CoPc to carbon nanotubes through covalent Co–O bonds has been shown to increase catalyst loading relative to physisorption[117]. Molecular catalysts can also be incorporated into the edges of graphene sheets. These graphite-conjugated catalysts (GCCs) are unique in that they place the catalyst in intimate electronic contact with the support. The electronic coupling between the catalyst and graphene sheets provides for a situation where they act as a single coherent system[120]. This situation fundamentally affects the redox demands of a single molecular catalysts and alters the reaction mechanism[121].

While the immobilization of molecular catalysts can impact on activity and selectivity, many of these investigations are performed in a batch setting and at very low current densities. It has therefore remained an open question as to how relevant these molecular systems are to commercial operation where higher current densities and a high pH range is required. These reasons have prompted research groups to start to investigate molecular catalysts in flow cell architectures[89,98,122,123]. Ren et al. found that immobilized CoPc in a flow cell operating at a current density of 150 mA/cm^2 could achieve a FE of 95%[122]. Zhuang and coworkers have since reported similar results at 200 mA/cm^2 with CoPc[89]. Both reports use a commercially relevant electrolyzer architecture: gaseous CO_2 is supplied to the cathodic GDE in a zero-gap flow cell with an AEM.

While it is unlikely that molecular CO_2RR catalysts will reach the stability needed for commercial viability, the number of variables available for tuning such catalysts are expected to advance the field. Molecular catalysts will undoubtedly provide insights into reaction mechanisms in the flow cell that would otherwise be difficult to resolve, but improvements in electrolyzer performance are also expected. For example, appending tetramethyl ammonium moieties on the macrocycle have already been shown to generate improvements in activity[98,124].

Although the activity of heterogeneous molecular CO2RR catalysts are much lower (≤ 100 A/gm) than solid-state catalysts (≤ 500 A/gm), the ligand environment enables the use of earth-abundant metals. Moreover, the mechanistic insights elucidated by well-defined molecular catalysts in turn can facilitate the rational design of the catalyst itself and the supporting material that improve both activity and stability. These strategies together with additional testing in the flow cell environment creates new opportunities to close the gap between molecular and solid-state catalysts[125.]

Highly dispersed single atom catalysts, especially those with metal-nitrogen sites in carbon substrates are also particularly attractive to the CO_2RR community because of their high conductivities, surface areas, maximum atom efficiencies and stabilities. The Wang, Strasser and Nam groups tested a Ni SAC-deposited GDE in flow cells[28,126,127]. They were able to obtain a current density of 380 mA/cm^2 with >90% selectivity in a three-compartment cell with flowing $KHCO_3$ electrolyte. No cell voltages were reported. This performance was reached with a strikingly high activity of >200 A/g. The system could be sustained at 200 mA/cm^2 for 20 h with a FE of 85%. The He group successfully synthesized a GDE with Ni SAC distributed throughout the carbon fiber support, maintaining 350 mA/cm² with 88% Faradaic efficiency for 120 h[128.] Bao and coworkers also reported the beneficial effects of combining a molecular catalyst (CoPc) and an iron-based SAC catalyst[129.] At this point we do not know whether SACs will be viable candidates for commercial CO_2 electrolyzers. A better assessment can be made after long term stability studies in zero gap cells are performed.

In summary then, the electrochemical conversion of CO_2 to CO is now reaching industrial performance. Industrially relevant currents and Faradaic efficiencies have already been achieved. Still, there are some areas that could use further improvement.

- Iridium free anode catalysts. Presently, all of the commercial CO_2 electrolysis cells use IrO_2 or $Ir_xRu_yO_2$ anode catalysts. Metal oxide and metal phosphide catalysts also show some activity[130], but when tested in commercial electrolyzers, the currents are much lower than those with the iridium based catalysts. MOF based catalysts[131] show high activity, but long term performance has not been achieved. Changing the ionomer to raise the pH to where iron and nickel are stable, has been tried. Unfortunately, CO_2 crossing through the membrane slowly lowers the pH, so the iron and nickel corrode in long term experiments. The worldwide supply of iridium is limited, and so alternatives to iridium are needed to allow CO_2 electrolysis to grow to the multi GW scale.
- Systems that convert CO_2 to CO at currents of ≥400 mA/cm² at cell potentials <2.5 V without KOH or other additives that need to be replaced. Present day catalysts start to produce CO at cell voltages as low as 1.5 V, but cell voltages of about 3 V are needed to obtain currents of 400 mA/cm². Lowering the voltage to below 2.5 V would open segments of the market that are uneconomic now.

- The use of bicarbonate feedstocks presents the opportunity to perform electrolysis where the reagent is regenerated by the CO_2 capture process[132]. This type of electrolysis bypasses the energy-intensive thermal regeneration steps to release CO_2 from the capture solution. This reactor, however, has a high cell voltage of ~3.5 V at 100 mA/cm^2 due to use of a bipolar membrane that dissociates water into H^+ and OH^-. More effort to lower cell voltages through membrane and reactor design are needed.

Production of formic acid

Next, we will discuss the electrochemical conversion of $CO_2 + H_2O$ into formic acid via the reactions:

$$CO_2 + H_2O + 2\,e^- \rightarrow HCOO^- + OH^-$$

$$H_2O \rightarrow \tfrac{1}{2}\,O_2 + 2H^+ + 2\,e^-$$

$$HCOO^- + H^+ \rightarrow HCOOH$$

$$OH^- + H^+ \rightarrow H_2O$$

Giving a net reaction:

$$CO_2 + H_2O \rightarrow HCOOH + \tfrac{1}{2}\,O_2$$

CO_2 electrolysis to produce formic acid has an equilibrium potential of 1.41 V, but as with the formation of CO, the optimum voltage is above 3 V. Dioxide Materials formic acid systems use a three compartment cell[6-8] which adds another 0.5-0.7 V.

Table 2 Performance of state of the art electrolyzers for the conversion of CO_2 and water to HCOOH

Electrolyzer current	>200 mA/cm^2
Catalyst activity	>50 A/gm
Initial Faradaic efficiency in an electrolyzer producing 2M formic acid	>80%
Faradaic efficiency loss at a constant current of 200 mA/cm^2 in an electrolyzer producing 2M formic acid	~10^{-4}/hr
Initial Faradaic efficiency in an electrolyzer producing <0.5 M formic acid	>90%
Turnovers demonstrated	>15,000,000
Single pass HCOOH concentration	2-5 mol/l

At present, production of formic acid via electrolysis is not as close to commercialization as CO production because of issues with catalyst stability[133,134] and selectivity[135]. The DMV/OCO group[136,137] found that they needed to reverse the potential to their cell every 2-10 hours to restore catalyst activity[137]. Dioxide Materials regenerates every 7-20 days. Unfortunately, the regeneration process is only partially successful; instead, the Faradaic efficiency drops with time. In a typical run producing 2-5 M formic acid in a Dioxide Materials CO_2 electrolyzer with a bismuth oxide catalyst shows an average Faradaic efficiency of about 80% for the first 100 hours but that might drop to about 75% in 500 hours, and to 65-70% in 1000 hours. XRD shows that bismuth oxide is being slowly converted to bismuth metal during the run. One can reverse the potential to partially oxidize bismuth metal back to bismuth oxide, but sufficient stability has not yet been achieved

Argawal et al.[138] found that their tin catalyst had a Faradaic efficiency of about 80% initially, but the selectivity dropped to about 70% after 120 hours. That can be improved by running at constant voltage. In that case the Faradaic efficiency was constant at about 70% through a 500 hour run, but the cell current dropped by 10% in 300 hours.

One can also achieve efficiencies above 90% by lowering the formic acid concentration produced by the electrolyzer to below 0.2 M. This eliminates the efficiency loss due to oxidation of the formic acid on the anode[135]. Unfortunately, such low concentrations are not practical commercially. Clearly, more work is needed to understand and eliminate the loss of efficiency.

Another issue is that formic acid is the preferred commercial product, but most papers on the electrochemical conversion of CO_2 to “formic acid” focus on the formation of formate salt and not formic acid. In 2017 Yang et al.[6-8] showed that in a 3-compartment cell design, one can do in situ acidification of the formate to yield a pure formic acid/water solution. The use of a Nafion cation exchange membrane significantly blocked the transport and oxidation of formic acid/formate ions at the anode. Xia et al.[10] extended the work to also include other oxygenates. The cathode pH is slightly acidic in the electrolyzers that produce formic acid directly, while the cathode pH is usually alkaline in the electrolyzers used to make formate salts. Care must be taken when trying to extrapolate results from alkaline conditions to the industrial situation.

Next, we wish to review what is known about bismuth oxide catalysts for the electrochemical conversion of CO_2 and water into formic acid. Bismuth oxide or oxyhalide nanocatalysts are the leading catalysts for electrochemical conversion of CO_2 and water to formic acid because they provide greater stability than the alternatives. Dioxide Materials commercial electrolyzers to convert CO_2 and water to formic acid use commercial bismuth oxide nanoparticles, but many other formulations seem to have promise.

So far, the highest currents are observed with bismuth oxyhalide catalysts. In 2018, He et al.[139] reported that pressured (5.6 Bar) electrolyzer with a strained bismuth catalyst made by electroreduction of bismuth oxychloride could produce formate with over 95% Faradaic efficiency at a current of 500 mA/cm². Garcia et at.[140] found similar results with bismuth prepared by electroreduction of bismuth oxybromide, while Liu et al.[141] reported similar results via bismuth catalysts produced from bismuth oxyiodide. All the published work using these catalysts was done under alkaline conditions, and no long term (>1000 hr) tests of these catalysts have yet been published. Dioxide Materials’ unpublished preliminary work indicates that bismuth oxyhalide catalysts have improved stability compared to bismuth oxide. So more work is needed. These results show that bismuth oxyhalide catalysts are very promising as catalysts for electrochemical formation of formic acid.

Bismuth nanosheets[142-149] also show promise. Xia et al.[10], tested a bismuth nanosheet catalyst in a 3-compartment cell producing formic acid. They reported an activity in the order of 500 A/gm of bismuth, and 100 hour stability at low currents (30 mA/cm^2).

There has also been work on formate formation on bismuth nanowires[150], bismuth nanotubes[151] and alloys of bismuth[152,153]. So far, none of the published work on these materials has been done using a cell design that can support high current. Consequently, the observed activity was an order of magnitude lower than those reported with commercially available bismuth oxide catalysts. It would be interesting to test these catalysts using a modern electrolyzer design[7].

In summary then, bismuth-based catalysts are presently the leading candidates as cathode catalysts for CO_2 conversion to formic acid. Commercially relevant catalyst activity has already been demonstrated but catalyst stability needs to be improved. In particular, a reduction in the rate of Faradaic efficiency loss to about 10^{-6}/hr at commercially relevant currents would greatly improve the prospects of the technology.

Tin based catalysts[8,9,138,154-158] are viable alternatives to the bismuth-based ones but so far they have shown lower stability and lower activity than the bismuth based catalysts. Commercially available tin oxide nanoparticles have been studied the most. Typical are the results of Lei et al.[156] who found that they could maintain Faradaic efficiencies over 70% for 3 hours if they ran at currents of 10 mA/cm^2. But the Faradaic efficiency dropped to about 20% at a cell current of 100 mA/cm^2. Argawal et al.[138] found that their tin catalyst had a Faradaic efficiency of about 80% at a current of 60 mA/cm^2 initially, but the Faradaic efficiency dropped to about 70% after 120 hours. Yang et. al[6-8] found that they could maintain over 80% Faradaic efficiency for 142 hours at a current of 140 mA/cm^2. Still, we are not aware of any examples where electrolyzers with tin nano-particle catalysts have exceeded the performance of bismuth catalysts under the same operating conditions.

There have been many attempts to improve the performance of tin by applying tin nanofibers[159], tin nanosheets[160,161], and tin alloys[162]. So far, the performance and stability of the tin catalysts has been lower than that of the bismuth based catalysts.

Many other metals have been tested for CO_2 conversion to formic acid. Lead, mercury, thallium, and cadmium are active, but they are not interesting commercially because of toxicity. The results on indium alloys are mixed[138,163-166]. Metal carbides[167], phosphides and transition metal oxides[168] have shown modest activity and stability, but so far the activity has been much less than that of the bismuth oxyhalides.

Various molecular and single atom catalysts have been used to produce formate from CO_2 at the bench scale. At this stage, there are no reports that can produce formic acid or formate at industrially relevant current densities (i.e., all reports are below 20 mA/cm^2). Meyer and Brookhart reported a modified Ir-pincer complex functionalized with a pyrene group immobilized on carbon nanotube through pi-pi interactions that can produce formate up to 15.6 mA/cm^2 with 83% selectivity[169]. Saveant and Robert reported that formate production was favored over CO when switching the metal center of metal-N_5 complex from Co to Fe in a homogeneous system.[170] Berben explored an Fe carbonyl cluster, $[Fe_4N(CO)_{12}]^-$ that can convert CO_2 to formate in an aqueous solution at 4 mA/cm^2 and selectivity of 96% for more than 24 hours.[171] It was found by the same group that the size of the secondary coordination sphere has an effect on the selectivity between HER and formate production[171]. Koper investigated the solvent effect for formate production using P4VP polymer encapsulated in protoporphyrins complexes with FE up to 70%[172,173]. Copper based MOF materials are also reported to serve as a precatalyst for CO_2-to-formate conversion with current density of ~5 mA/cm^2 and $FE_{formate}$ 68.4% [174]. Positively charged single-atom $Sn^{\delta+}$ on N-doped graphene is able to conduct CO_2-to-formate conversion at the current of 11.7 mA/cm^2 and 74.3% selectivity with an outstanding stability of 200 h[175]. The authors attribute this performance to the positively charged $Sn^{\delta+}$ sites stabilizing the reaction intermediates such as $CO_2^{\bullet-}$. These performances suggest achievement of industrial relevant current for CO_2 to formate with single atom and organometallic catalysts in a flow cell is potentially viable.

Processes for the Production of C_2 products

Table 3 A comparison of the one-step and two-step process for CO_2 conversion to C_2 products

	One Step Process	Two Step
Preferred application	Modest scale C_2 production	Commodity scale C_2 production
Key advantage	Simpler process	Lower energy use Base metal anode catalysts
Key disadvantage	Higher energy use	More complex process

The results above show that CO_2 can be readily converted to CO or HCOOH in an electrolyzer. In the last several years, there has also been interest in converting CO_2 to C_2 products electrochemically. There are three approaches:

- A one step approach, where all the chemistry occurs in a single electrolyzer, and
- A two-step approach where CO_2 is converted to CO ($+O_2$) in the first electrolyzer and then CO is hydrogenated to C_2 products in a second electrolyzer.
- A hybrid approach [12,176,177] where a silver or gold catalyst active for CO_2 conversion to CO and copper catalyst active for the production of C_2 products were placed in a single electrolyzer.

Each process has advantages for different applications. If one is adding a CO_2 electrolyzer to a Gen I ethanol biorefinery, the one step process is of advantage, because one needs fewer process units. On the other hand, if one wanted to produce millions of tons per year of a C_2 product, one would choose the two-step process because the electricity costs are lower. Further, the capital expenditures can be lower, since one can circulate KOH through the anode, and use base metal anode catalysts – although that does require one to remove unreacted CO_2 from the output of the first electrolyzer.

The two-step process for the conversion of CO_2 to C_2 products was first discussed by Hori et al.[178,179] in 1997. But Hori's early papers have not been well cited, and the application seems to have been forgotten for many years. More recently, a number of papers have been published on the topic[18-23,180-193] as reviewed by Jouny et al.[20]. Generally, the approach is to first convert the CO_2 to CO electrochemically using a gold or silver catalyst as described in section 2. Next a copper catalyst is used to electrochemically hydrogenate the CO to C_2 products such as ethylene or ethanol[20]. Zhang et al.[23] has reviewed the electrochemical hydrogenation of CO on copper. The results depend strongly on the morphology of the catalyst[182,183], the potential, and pH[190]. As a result, the reproducibility from one laboratory to the next has not been wonderful. At this point, the two-step process for CO_2 conversion to C_2 and higher products has considerable potential, the systems are not ready for industrial deployment. Key needs include:

- Stable, reproducible catalysts that do not change during operation. Jung et al. [194] found that the morphology of copper catalysts change the electrochemical reduction of CO_2. On-off operation or voltage cycling also changes the morphology of copper catalysts[195-197]. Feng et al[182] and Luc et al.[183] found that morphology changes lead to selectivity changes so one would expect the effects to be significant.
- Adding adsorbates[198,199] or cages[184,200] to further control the selectivity. These approaches are used in the one step process, but they have barely been explored for the two-step process.

- Long term tests to verify performance for thousands of hours.

The one step process is an alternative to the two-step process described earlier. Progress has been recently reviewed by Fan at al.[201] In this case the activation of CO_2 to form a CO intermediate and the hydrogenation of the CO to HCO, and subsequent C-C bond formation occurs on the same catalyst. So, while the one step process has less process complexity, it does require a more complex catalyst.

Copper is the best catalyst for CO_2 conversion to C_2 products, but suffers from two weaknesses:

- CO_2 electrolysis on clean copper produces CO and C_2 products, but the Faradaic efficiency is low. Instead the main product is hydrogen. One needs to reduce the rate of hydrogen formation or the Faradaic efficiency for C_2 will be too small for practical applications.
- The rate of the first step in the process, CO_2 conversion to CO is low on clean copper. One needs to add a second catalyst for CO_2 to CO conversion process, if one wants to achieve an industrially significant rate.

In 2002, Yano et al.[202] reported that ethylene could form during CO_2 electrolysis on a carbon coated copper catalyst. In the initial work, hydrogen was the major reaction product, but by 2004, Yano et al.[203] showed that they could reduce CO_2 to ethylene with near 80% Faradaic efficiency at 11 mA/cm² current, by running the reaction in 3 M KBr. Yano postulated that the combination of the porous carbon layer and the adsorbed halides had suppressed hydrogen formation leading to the high Faradaic efficiency.

There have been hundreds of papers on the one step process since 2004, as summarized by Kuhl et al.[204] and Zhao et al.[205] but most showed lower cell currents and efficiencies than Yano et al.[203].

Recently some papers have shown results that equal or exceed those in Yano's work, however.[11-17,199,206-208] For example, Zhu et al.[11] found that they could produce ethanol and acetic acid on a nanostructured copper catalyst, and their Faradaic efficiency equaled that of Yano et al. (80%) at 11 mA/cm² provided KCl was used to suppress hydrogen formation. Li et al.[12] and Hoang et al.[209] were able to raise the cell current in a cell producing ethanol to 124 and 300 mA/cm² respectively by adding a second catalyst that was active for conversion of CO_2 to CO, albeit at reduced faradaic efficiency since not hydrogen suppression was done. Wang et at al[14]raised the Faradaic efficiency to 52% by using KOH to partially suppress the H_2 formation. García de Arquer et al.[13] raised the current to 912 mA/cm² by running in a pressurized cell. Also interesting morphology effects have been seen as summarized by De Gregorio et al.[206] and carbon overlayers and other hydrocarbons[199] can be used to improve selectivity.

Table 4 summarizes key results in this area. Generally, the highest currents and selectivities are seen when KOH is used as an electrolyte, but KOH is not a preferred electrolyte for commercial cells. There are two issues: i) KOH readily reacts with CO_2 to form stable carbonates, so the KOH would need to be continuously replaced. ii) the copper catalysts have limited stability in alkaline solutions[210]. While the copper is stable at the applied potential in the cell, the copper quickly oxidizes when the potential is removed[210]. The oxidation makes practical operation difficult.

KCl and KBr have similar issues in that Cl^- and Br^- will react on the anode to produce Cl_2, Br_2 respectively and OH^-. Again, continuous replacement will be needed. $KHCO_3$ is better in that it is relatively stable under the conditions in the electrolyzer, and copper corrosion is reduced[199], but the performance is lower.

At this point no one has demonstrated both industrially relevant currents (i.e. >200 mA/cm^2) and Faradaic efficiencies (>60%) without using KOH or a potassium halide.

Table 4 Performance of state of the art electrolyzers for the conversion of CO_2 and water to C_2 products.

		Electrolyte
Total Faradaic efficiency to all C_2 products at currents <20 mA/cm^2	80%[11,203]	KBr, KCl
Total Faradaic efficiency to all C_2 products at currents >100 mA/cm^2	83%[14]	KOH
Faradaic efficiency to ethanol at currents <20 mA/cm^2	63%[11]	KCl
Faradaic efficiency to ethanol at currents >100 mA/cm^2	52%[14]	KOH
	41%	$KHCO_3$
Faradaic efficiency to ethylene at currents <20 mA/cm^2	80%[203]	KBr
Faradaic efficiency to ethylene at currents >100 mA/cm^2	80%[15]	KOH
Highest cell current observed	1 A/cm^2 [13]	KOH

Ligands to improve reaction selectivity

Before we close, we also wanted to note that there is a significant opportunity to use ligands to improve the selectivity and activity of CO_2 reduction catalysts[46,54,81,211-220]. Years ago, Rosen et al.[218,219] found that the addition of an imidazole based ion liquid lowered the overpotential for the reaction and raised the faradaic efficiency. More recently, ligands have been shown to modify the electron density of the reactive metal site[200,211], change the crystal faces that are exposed in nanoparticles[81,195,221,222] tune the binding strength of intermediates[12,220], block side reactions[46,213,223,224], aid assembly of the nanostructures[198], and act as a co-catalyst[209,212,213,216,221,222,225]. These effects are similar to those observed with organometallic compounds[97]. So far, no one has published work on modifying the secondary coordination sphere, but unpublished work found that such modifications can improve the reaction rate.

Still, there is much more work to be done. We do not know, for example whether the ligands that are known to aid CO_2 electrolysis on organometallic compounds[97] are also useful when the ligands are bound to metal nanoparticles. Systematic studies of the effects of ligand structure on nanocatalyst performance has not been published. There is mechanistic work on the effects of imidazoliums on catalyst performance[226,227], but little information about other ligands. Clearly, further work on the effects of ligands on CO_2 electrolysis would make an important contribution to the field.

Summary

In summary, in the last 5 years, the electrochemical conversion of CO_2 has switched from a laboratory curiosity to a commercially viable process. Lab scale electrolyzers are already being sold. Pilot units are moving toward commercialization. Better nanocatalysts, and better reactor designs have been key components of the advances, but each reaction is different. In the case of CO_2 conversion to CO, controlling the particle size, and the use of gas diffusion electrodes seems to be key to achieving state of the art performance. In the case of CO_2 conversion to formic acid, catalysts that stabilize the metal oxide are key. State of the art methods for the conversion of CO_2

+ H_2O to ethylene or ethanol requires cocatalysts to enhance the conversion of CO_2 to CO, and additives to block hydrogen formation. Each of these processes are areas of ongoing research, and we expect many advances in the future.

Literature cited

1 Siemens. *Press Release CO_2 for a clean performance: Rheticus research project enters phase 2* <https://press.siemens.com/global/en/pressrelease/research-project-rheticus> (2019).

2 Krause, R. *et al.* Industrial Application Aspects of the Electrochemical Reduction of CO_2 to CO in Aqueous Electrolyte. *Chem. Ing. Tech.* **92**, 53-61, doi:10.1002/cite.201900092 (2020).

3 Haas, T., Krause, R., Weber, R., Demler, M. & Schmid, G. Technical photosynthesis involving CO_2 electrolysis and fermentation. *Nature Catalysis* **1**, 32-39, doi:10.1038/s41929-017-0005-1 (2018).

4 Matthews, T. S. *et al.* On the route to commercialization of a CO_2 electrolyzer: lessons learned from an industry effort to fight climate change. *Prepr. - Am. Chem. Soc., Div. Energy Fuels* **60**, 222-223 (2015).

5 Kaczur, J. J., Yang, H., Liu, Z., Sajjad, S. D. & Masel, R. I. A Review of the Use of Immobilized Ionic Liquids in the Electrochemical Conversion of CO_2 *J.. Carbon Research* **6**, 33, doi:10.3390/c6020033 (2020).

6 Kaczur, J. J., Yang, H., Liu, Z., Sajjad, S. D. & Masel, R. I. Carbon dioxide and water electrolysis using new alkaline stable anion membranes. *Front. Chem.* **6**, 263/261-263/216, doi:10.3389/fchem.2018.00263 (2018).

7 Yang, H., Kaczur, J. J., Sajjad, S. D. & Masel, R. I. Electrochemical conversion of CO_2 to formic acid utilizing Sustainion membranes. *J. CO2 Util.* **20**, 208-217, doi:10.1016/j.jcou.2017.04.011 (2017).

8 Kaczur, J. J., Yang, H., Sajjad, S. D. & Masel, R. I. Method and System for Electrochemical Production of Formic Acid from Carbon Dioxide, US Patent. 10047446 (2018).

9 Yang, H., Kaczur, J. J., Sajjad, S. D. & Masel, R. I. CO_2 conversion to formic acid in a three compartment cell with sustainion membranes. *ECS Trans.* **77**, 1425-1431, doi:10.1149/07711.1425ecst (2017).

10 Xia, C. *et al.* Continuous production of pure liquid fuel solutions via electrocatalytic CO2 reduction using solid-electrolyte devices. *Nat. Energy* **4**, 776-785, doi:10.1038/s41560-019-0451-x (2019).

11 Zhu, Q. *et al.* Carbon dioxide electroreduction to C2 products over copper-cuprous oxide derived from electrosynthesized copper complex. *Nat. Commun.* **10**, 1-11, doi:10.1038/s41467-019-11599-7 (2019).

12 Li, F. *et al.* Cooperative CO_2-to-ethanol conversion via enriched intermediates at molecule–metal catalyst interfaces. *Nature Catalysis* **3**, 75-82, doi:10.1038/s41929-019-0383-7 (2020).

13 García de Arquer, F. P. *et al.* CO_2; electrolysis to multicarbon products at activities greater than 1 A /cm^2. *Science* **367**, 661, doi:10.1126/science.aay4217 (2020).

14 Wang, X. *et al.* Efficient electrically powered CO_2-to-ethanol via suppression of deoxygenation. *Nature Energy*, doi:10.1038/s41560-020-0607-8 (2020).

15 Zhong, M. *et al.* Accelerated discovery of CO_2 electrocatalysts using active machine learning. *Nature* **581**, 178-183, doi:10.1038/s41586-020-2242-8 (2020).

16 Dinh, C.-T. *et al.* CO_2 electroreduction to ethylene via hydroxide-mediated copper catalysis at an abrupt interface. *Science* **360**, 783, doi:10.1126/science.aas9100 (2018).

17 Vennekoetter, J.-B., Scheuermann, T., Sengpiel, R. & Wessling, M. The electrolyte

matters: Stable systems for high rate electrochemical CO_2 reduction. *J. CO2 Util.* **32**, 202-213, doi:10.1016/j.jcou.2019.04.007 (2019).
18 Romero Cuellar, N. S. *et al.* Two-step electrochemical reduction of CO_2 towards multi-carbon products at high current densities. *Journal of CO2 Utilization* **36**, 263-275, doi:10.1016/j.jcou.2019.10.016 (2020).
19 Romero Cuellar, N. S., Wiesner-Fleischer, K., Fleischer, M., Rucki, A. & Hinrichsen, O. Advantages of CO over CO_2 as reactant for electrochemical reduction to ethylene, ethanol and n-propanol on gas diffusion electrodes at high current densities. *Electrochim. Acta* **307**, 164-175, doi:10.1016/j.electacta.2019.03.142 (2019).
20 Jouny, M., Hutchings, G. S. & Jiao, F. Carbon monoxide electroreduction as an emerging platform for carbon utilization. *Nat. Catal.* **2**, 1062-1070, doi:10.1038/s41929-019-0388-2 (2019).
21 Li, C. W., Ciston, J. & Kanan, M. W. Electroreduction of carbon monoxide to liquid fuel on oxide-derived nanocrystalline copper. *Nature (London, U. K.)* **508**, 504-507, doi:10.1038/nature13249 (2014).
22 Gurudayal *et al.* Sequential Cascade Electrocatalytic Conversion of Carbon Dioxide to C-C Coupled Products. *ACS Appl. Energy Mater.* **2**, 4551-4559, doi:10.1021/acsaem.9b00791 (2019).
23 Zhang, H., Li, J., Cheng, M.-J. & Lu, Q. CO Electroreduction: Current Development and Understanding of Cu-Based Catalysts. *ACS Catal.* **9**, 49-65, doi:10.1021/acscatal.8b03780 (2019).
24 Ren, S. *et al.* Molecular electrocatalysts can mediate fast, selective CO2 reduction in a flow cell. *Science* **365**, 367-369 (2019).
25 Wang, Q., Zhang, Y., Lin, H. & Zhu, J. Recent Advances in Metal-Organic Frameworks for Photo-/Electrocatalytic CO_2 Reduction. *Chem. - Eur. J.* **25**, 14026-14035, doi:10.1002/chem.201902203 (2019).
26 Zhang, E. *et al.* Bismuth Single Atoms Resulting from Transformation of Metal-Organic Frameworks and Their Use as Electrocatalysts for CO_2 Reduction. *J. Am. Chem. Soc.* **141**, 16569-16573, doi:10.1021/jacs.9b08259 (2019).
27 Jeong, H.-Y. *et al.* Achieving highly efficient CO_2 to CO electroreduction exceeding 300 mA cm-2 with single-atom nickel electrocatalysts. *J. Mater. Chem. A* **7**, 10651-10661, doi:10.1039/c9ta02405k (2019).
28 Zheng, T. *et al.* Large-Scale and Highly Selective CO_2 Electrocatalytic Reduction on Nickel Single-Atom Catalyst. *Joule* **3**, 265-278, doi:10.1016/j.joule.2018.10.015 (2019).
29 Li, J., Zhang, Y. & Kornienko, N. Heterogeneous electrocatalytic reduction of CO_2 promoted by secondary coordination sphere effects. *New Journal of Chemistry*, doi:10.1039/C9NJ05892C (2020).
30 Ovalle, V. J. & Waegele, M. M. Understanding the Impact of N-Arylpyridinium Ions on the Selectivity of CO_2 Reduction at the Cu/Electrolyte Interface. *J. Phys. Chem. C* **123**, 24453-24460, doi:10.1021/acs.jpcc.9b08666 (2019).
31 Sinha, S. & Warren, J. J. Unexpected Solvent Effect in Electrocatalytic CO_2 to CO Conversion Revealed Using Asymmetric Metalloporphyrins. *Inorg. Chem.* **57**, 12650-12656, doi:10.1021/acs.inorgchem.8b01814 (2018).
32 Shen, J., Lan, D. & Yang, T. Influence of supporting electrolyte on the electrocatalysis of CO_2 reduction by cobalt protoporphyrin. *Int. J. Electrochem. Sci.* **13**, 9847-9857, doi:10.20964/2018.10.62 (2018).

33 Zhao, M. *et al.* Inhibiting Hydrogen Evolution using a Chloride Adlayer for Efficient Electrochemical CO_2 Reduction on Zn Electrodes. *ACS Appl Mater Interfaces* **12**, 4565-4571, doi:10.1021/acsami.9b22811 (2020).

34 Yoshida, T. *et al.* Ionic-caged heterometallic bismuth-platinum complex exhibiting electrocatalytic CO_2 reduction. *Dalton Trans.* **49**, 2652-2660, doi:10.1039/c9dt04817k (2020).

35 Suter, S. & Haussener, S. Optimizing mesostructured silver catalysts for selective carbon dioxide conversion into fuels. *Energy Environ. Sci.* **12**, 1668-1678, doi:10.1039/c9ee00656g (2019).

36 Pankhurst, J. R., Guntern, Y. T., Mensi, M. & Buonsanti, R. Molecular tunability of surface-functionalized metal nanocrystals for selective electrochemical CO_2 reduction. *Chem. Sci.* **10**, 10356-10365, doi:10.1039/c9sc04439f (2019).

37 Ross, M. B. *et al.* Designing materials for electrochemical carbon dioxide recycling. *Nat. Catal.* **2**, 648-658, doi:10.1038/s41929-019-0306-7 (2019).

38 Xie, J., Huang, Y., Wu, M. & Wang, Y. Electrochemical Carbon Dioxide Splitting. *ChemElectroChem* **6**, 1587-1604, doi:10.1002/celc.201801716 (2019).

39 Song, J. T., Song, H., Kim, B. & Oh, J. Towards higher rate electrochemical CO_2 conversion: from liquid-phase to gas-phase systems. *Catalysts* **9**, 224/221-224/225, doi:10.3390/catal9030224 (2019).

40 Li, F., MacFarlane, D. R. & Zhang, J. Recent advances in the nanoengineering of electrocatalysts for CO_2 reduction. *Nanoscale* **10**, 6235-6260, doi:10.1039/C7NR09620H (2018).

41 Nwabara, U. O., Cofell, E. R., Verma, S., Negro, E. & Kenis, P. J. A. Durable Cathodes and Electrolyzers for the Efficient Aqueous Electrochemical Reduction of CO_2. *ChemSusChem* **13**, 855-875, doi:10.1002/cssc.201902933 (2020).

42 Lee, M.-Y. *et al.* Current achievements and the future direction of electrochemical CO_2 reduction: A short review. *Critical Reviews in Environmental Science and Technology* **50**, 769-815, doi:10.1080/10643389.2019.1631991 (2020).

43 Christensen, R., Hansen, H. A. & Vegge, T. Identifying systematic DFT errors in catalytic reactions. *Catalysis Science & Technology* **5**, 4946-4949, doi:10.1039/C5CY01332A (2015).

44 Yoo, J. S., Christensen, R., Vegge, T., Norskov, J. K. & Studt, F. Theoretical Insight into the Trends that Guide the Electrochemical Reduction of Carbon Dioxide to Formic Acid. *ChemSusChem* **9**, 358-363, doi:10.1002/cssc.201501197 (2016).

45 Studt, F., Abild-Pedersen, F., Varley, J. B. & Nørskov, J. K. CO and CO_2 Hydrogenation to Methanol Calculated Using the BEEF-vdW Functional. *Catalysis Letters* **143**, 71-73, doi:10.1007/s10562-012-0947-5 (2013).

46 Liu, Z., Yang, H., Kutz, R. & Masel, R. I. CO_2 electrolysis to CO and O2 at high selectivity, stability and efficiency using Sustainion membranes. *J. Electrochem. Soc.* **165**, J3371-J3377, doi:10.1149/2.0501815jes (2018).

47 Edwards, J. P. *et al.* Efficient electrocatalytic conversion of carbon dioxide in a low-resistance pressurized alkaline electrolyzer. *Appl. Energy* **261**, 114305, doi:10.1016/j.apenergy.2019.114305 (2020).

48 Masel, R. I., Chen, Q., Liu, Z. & Kutz, R. Catalyst Layers and electrolyzers, U.S. Patent. 9481939 (2018).

49 Masel, R. I., Liu, Z., Kutz, R. & Sajjad, S. D. Catalyst Layers and Electrolyzers, U. S. Patent
9,945,040 (2018).

50 Higgins, D., Hahn, C., Xiang, C., Jaramillo, T. F. & Weber, A. Z. Gas-Diffusion Electrodes for Carbon Dioxide Reduction: A New Paradigm. *ACS Energy Lett.* **4**, 317-324, doi:10.1021/acsenergylett.8b02035 (2019).

51 Endrődi, B. *et al.* Multilayer Electrolyzer Stack Converts Carbon Dioxide to Gas Products at High Pressure with High Efficiency. *ACS Energy Letters* **4**, 1770-1777, doi:10.1021/acsenergylett.9b01142 (2019).

52 Liu, Z. *et al.* Electrochemical generation of syngas from water and carbon dioxide at industrially important rates. *J. CO2 Util.* **15**, 50-56, doi:10.1016/j.jcou.2016.04.011 (2016).

53 Ma, C. *et al.* Carbon nanotubes with rich pyridinic nitrogen for gas phase CO_2 electroreduction. *Appl. Catal., B* **250**, 347-354, doi:10.1016/j.apcatb.2019.03.041 (2019).

54 Kutz, R. B. *et al.* Sustainion Imidazolium-Functionalized Polymers for Carbon Dioxide Electrolysis. *Energy Technol. (Weinheim, Ger.)* **5**, 929-936, doi:10.1002/ente.201600636 (2017).

55 Masel, R. I., Chen, Q. & Liu, Z. Ion-Conducting Membranes, U.S. Patent 9,849,450 (2017).

56 Masel, R. I., Chen, Q., Liu, Z. & Kutz, R. Ion-Conducting Membranes, U.S. Patent 9,370,773 (2016).

57 Landes, H., Sanchis, E. M. F. & Hanebuth, M. Method and device for the electrochemical utilization of carbon dioxide, European patent application. EP3414363A1 (2018).

58 Krause, R., Neubauer, S., Reller, C., Schmid, B. & Schmid, G. CO_2 electrolysis method. WO2018050419A1 (2018).

59 Verma, S., Lu, X., Kenis, P. J. A., Ma, S. & Masel, R. I. The effect of electrolyte composition on the electroreduction of CO_2 to CO on Ag based gas diffusion electrodes. *Phys Chem Chem Phys* **18**, 7075-7084, doi:10.1039/C5CP05665A (2016).

60 Salehi-Khojin, A. *et al.* Nanoparticle Silver Catalysts That Show Enhanced Activity for Carbon Dioxide Electrolysis. *J. Phys. Chem. C* **117**, 1627-1632, doi:10.1021/jp310509z (2013).

61 Masel, R. I., Salahi-Khogin, A. & Rosen, B. Catalysts for electrochemical conversion of carbon dioxide, U.S. Patent. 9,012,345 (2015).

62 Kim, C. *et al.* Achieving Selective and Efficient Electrocatalytic Activity for CO_2 Reduction Using Immobilized Silver Nanoparticles. *Journal of the American Chemical Society* **137**, 13844-13850, doi:10.1021/jacs.5b06568 (2015).

63 Zhang, L., Zhao, Z.-J. & Gong, J. Nanostructured Materials for Heterogeneous Electrocatalytic CO_2 Reduction and their Related Reaction Mechanisms. *Angewandte Chemie International Edition* **56**, 11326-11353, doi:10.1002/anie.201612214 (2017).

64 Zhu, W. *et al.* Monodisperse Au Nanoparticles for Selective Electrocatalytic Reduction of CO_2 to CO. *Journal of the American Chemical Society* **135**, 16833-16836, doi:10.1021/ja409445p (2013).

65 Cho, M. *et al.* Versatile, transferable 3-dimensionally nanofabricated Au catalysts with high-index crystal planes for highly efficient and robust electrochemical CO_2 reduction. *J. Mater. Chem. A* **7**, 6045-6052, doi:10.1039/c8ta12242c (2019).

66 Mistry, H. *et al.* Exceptional Size-Dependent Activity Enhancement in the Electroreduction of CO_2 over Au Nanoparticles. *J. Am. Chem. Soc.* **136**, 16473-16476, doi:10.1021/ja508879j (2014).

67 Weekes, D. M., Salvatore, D. A., Reyes, A., Huang, A. & Berlinguette, C. P. Electrolytic CO_2 Reduction in a Flow Cell. *Acc. Chem. Res.* **51**, 910-918, doi:10.1021/acs.accounts.8b00010 (2018).

68 Mahyoub, S. A. *et al.* An overview on the recent developments of Ag-based electrodes in

the electrochemical reduction of CO_2 to CO. *Sustainable Energy Fuels* **4**, 50, doi:10.1039/c9se00594c (2019).
69 Sun, D. *et al.* Rational Design of Ag-Based Catalysts for the Electrochemical CO_2 Reduction to CO: A Review. *ChemSusChem* **13**, 39-58, doi:10.1002/cssc.201902061 (2020).
70 Rudnev, A. V. *et al.* Enhanced electrocatalytic CO formation from CO_2 on nanostructured silver foam electrodes in ionic liquid/water mixtures. *Electrochim. Acta* **306**, 245-253, doi:10.1016/j.electacta.2019.03.102 (2019).
71 Liu, S.-Q. *et al.* Hollow porous Ag spherical catalysts for highly efficient and selective electrocatalytic reduction of CO_2 to CO. *ACS Sustainable Chem. Eng.* **7**, 14443-14450, doi:10.1021/acssuschemeng.9b01635 (2019).
72 Kottakkat, T. *et al.* Electrodeposited AgCu Foam Catalysts for Enhanced Reduction of CO_2 to CO. *ACS Appl. Mater. Interfaces* **11**, 14734-14744, doi:10.1021/acsami.8b22071 (2019).
73 Wang, Y., Niu, C. & Zhu, Y. Copper-silver bimetallic nanowire arrays for electrochemical reduction of carbon dioxide. *Nanomaterials* **9**, 173, doi:10.3390/nano9020173 (2019).
74 Lee, S., Park, G. & Lee, J. Importance of Ag-Cu Biphasic Boundaries for Selective Electrochemical Reduction of CO_2 to Ethanol. *ACS Catal.* **7**, 8594-8604, doi:10.1021/acscatal.7b02822 (2017).
75 Hoang, T. T. H. *et al.* Nanoporous Copper-Silver Alloys by Additive-Controlled Electrodeposition for the Selective Electroreduction of CO_2 to Ethylene and Ethanol. *J. Am. Chem. Soc.* **140**, 5791-5797, doi:10.1021/jacs.8b01868 (2018).
76 Hjorth, I., Nord, M., Roenning, M., Yang, J. & Chen, D. Electrochemical reduction of CO_2 to synthesis gas on CNT supported $Cu_xZn_{1-x}O$ catalysts. *Catal. Today*, Ahead of Print, doi:10.1016/j.cattod.2019.02.045 (2019).
77 Lin, R. *et al.* PdAg bimetallic electrocatalyst for highly selective reduction of CO_2 with low COOH* formation energy and facile CO desorption. *Nano Res.* **12**, 2866-2871, doi:10.1007/s12274-019-2526-1 (2019).
78 Zeng, J. *et al.* Pd-Ag Alloy Electrocatalysts for CO_2 Reduction: Composition Tuning to Break the Scaling Relationship. *ACS Appl. Mater. Interfaces* **11**, 33074-33081, doi:10.1021/acsami.9b11729 (2019).
79 Larrazabal, G. O., Martin, A. J., Mitchell, S., Hauert, R. & Perez-Ramirez, J. Synergistic effects in silver-indium electrocatalysts for carbon dioxide reduction. *J. Catal.* **343**, 266-277, doi:10.1016/j.jcat.2015.12.014 (2016).
80 Park, H. *et al.* AgIn dendrite catalysts for electrochemical reduction of CO_2 to CO. *Appl. Catal., B* **219**, 123-131, doi:10.1016/j.apcatb.2017.07.038 (2017).
81 Abeyweera, S. C., Yu, J., Perdew, J. P., Yan, Q. & Sun, Y. Hierarchically 3D Porous Ag Nanostructures Derived from Silver Benzenethiolate Nanoboxes: Enabling CO_2 Reduction with a Near-Unity Selectivity and Mass-Specific Current Density over 500 A/g. *Nano Letters* **20**, 2806-2811, doi:10.1021/acs.nanolett.0c00518 (2020).
82 Lee, W. H. *et al.* Highly selective and scalable CO2 to CO - Electrolysis using coral-nanostructured Ag catalysts in zero-gap configuration. *Nano Energy*, 105030, doi:https://doi.org/10.1016/j.nanoen.2020.105030 (2020).
83 Jhong, H.-R. M. *et al.* Gold Nanoparticles on Polymer-Wrapped Carbon Nanotubes: An Efficient and Selective Catalyst for the Electroreduction of CO_2. *ChemPhysChem* **18**, 3274-3279, doi:10.1002/cphc.201700815 (2017).
84 Verma, S. *et al.* Insights into the Low Overpotential Electroreduction of CO_2 to CO on a

Supported Gold Catalyst in an Alkaline Flow Electrolyzer. *ACS Energy Lett.* **3**, 193-198, doi:10.1021/acsenergylett.7b01096 (2018).

85 Jin, L. *et al.* Ultrasmall Au nanocatalysts supported on nitrided carbon for electrocatalytic CO_2 reduction: the role of the carbon support in high selectivity. *Nanoscale* **10**, 14678-14686, doi:10.1039/C8NR04322A (2018).

86 Hong, S., Lee, S., Kim, S., Lee, J. K. & Lee, J. Anion dependent CO/H_2 production ratio from CO_2 reduction on Au electrocatalyst. *Catal. Today* **295**, 82-88, doi:10.1016/j.cattod.2017.05.063 (2017).

87 Goyal, A., Marcandalli, G., Mints, V. A. & Koper, M. T. M. Competition between CO2 Reduction and Hydrogen Evolution on a Gold Electrode under Well-Defined Mass Transport Conditions. *J. Am. Chem. Soc.* **142**, 4154-4161, doi:10.1021/jacs.9b10061 (2020).

88 Zhang, B. A., Ozel, T., Elias, J. S., Costentin, C. & Nocera, D. G. Interplay of Homogeneous Reactions, Mass Transport, and Kinetics in Determining Selectivity of the Reduction of CO_2 on Gold Electrodes. *ACS Cent. Sci.* **5**, 1097-1105, doi:10.1021/acscentsci.9b00302 (2019).

89 Yin, Z. *et al.* An alkaline polymer electrolyte CO2 electrolyzer operated with pure water. *Energy & Environmental Science* **12**, 2455-2462, doi:10.1039/C9EE01204D (2019).

90 Zhu, W. *et al.* Active and Selective Conversion of CO_2 to CO on Ultrathin Au Nanowires. *J. Am. Chem. Soc.* **136**, 16132-16135, doi:10.1021/ja5095099 (2014).

91 Wen, X. *et al.* A reassembled nanoporous gold leaf electrocatalyst for efficient CO_2 reduction towards CO. *Inorg. Chem. Front.* **5**, 1207-1212, doi:10.1039/C8QI00023A (2018).

92 Chen, Y., Li, C. W. & Kanan, M. W. Aqueous CO_2 Reduction at Very Low Overpotential on Oxide-Derived Au Nanoparticles. *Journal of the American Chemical Society* **134**, 19969-19972, doi:10.1021/ja309317u (2012).

93 Ismail, A. M., Csapo, E. & Janaky, C. Correlation between the work function of Au-Ag nanoalloys and their electrocatalytic activity in carbon dioxide reduction. *Electrochim. Acta* **313**, 171-178, doi:10.1016/j.electacta.2019.05.016 (2019).

94 Wu, N., Xiao, L. & Zhuang, L. Theoretical search for novel Au or Ag bimetallic alloys capable of transforming CO_2 into hydrocarbons. *J. Mater. Chem. A* **7**, 20567-20573, doi:10.1039/c9ta07929g (2019).

95 Xiang, H. *et al.* Copper-Indium Binary Catalyst on a Gas Diffusion Electrode for High-Performance CO_2 Electrochemical Reduction with Record CO Production Efficiency. *ACS Appl. Mater. Interfaces* **21**, 601-608, doi:10.1021/acsami.9b16862 (2020).

96 Chen, D. *et al.* Tailoring the Selectivity of Bimetallic Copper-Palladium Nanoalloys for Electrocatalytic Reduction of CO_2 to CO. *ACS Appl. Energy Mater.* **1**, 883-890, doi:10.1021/acsaem.7b00320 (2018).

97 Francke, R., Schille, B. & Roemelt, M. Homogeneously Catalyzed Electroreduction of Carbon Dioxide—Methods, Mechanisms, and Catalysts. *Chemical Reviews* **118**, 4631-4701, doi:10.1021/acs.chemrev.7b00459 (2018).

98 Torbensen, K. *et al.* Molecular Catalysts Boost the Rate of Electrolytic CO2 Reduction. *ACS Energy Letters* **5**, 1512-1518, doi:10.1021/acsenergylett.0c00536 (2020).

99 Corbin, N., Zeng, J., Williams, K. & Manthiram, K. Heterogeneous molecular catalysts for electrocatalytic CO2 reduction. *Nano Research* **12**, 2093-2125, doi:10.1007/s12274-019-2403-y (2019).

100 Sun, L., Reddu, V., Fisher, A. C. & Wang, X. Electrocatalytic reduction of carbon dioxide: opportunities with heterogeneous molecular catalysts. *Energy & Environmental Science*

13, 374-403, doi:10.1039/C9EE03660A (2020).
101 Choi, J. *et al.* Steric Modification of a Cobalt Phthalocyanine/Graphene Catalyst To Give Enhanced and Stable Electrochemical CO_2 Reduction to CO. *ACS Energy Lett.* **4**, 666-672, doi:10.1021/acsenergylett.8b02355 (2019).
102 Chen, J. *et al.* Facile synthesis of polymerized cobalt phthalocyanines for highly efficient CO_2 reduction. *Green Chem.* **21**, 6056-6061, doi:10.1039/c9gc02705j (2019).
103 Rotundo, L. *et al.* Electrochemical CO2 reduction in water at carbon cloth electrodes functionalized with a fac-Mn(apbpy)(CO)3Br complex. *Chemical Communications* **55**, 775-777, doi:10.1039/C8CC08385A (2019).
104 Hu, X.-M., Rønne, M. H., Pedersen, S. U., Skrydstrup, T. & Daasbjerg, K. Enhanced Catalytic Activity of Cobalt Porphyrin in CO2 Electroreduction upon Immobilization on Carbon Materials. *Angewandte Chemie International Edition* **56**, 6468-6472, doi:10.1002/anie.201701104 (2017).
105 He, L., Sun, X., Zhang, H. & Shao, F. G-quadruplex Nanowires To Direct the Efficiency and Selectivity of Electrocatalytic CO2 Reduction. *Angewandte Chemie International Edition* **57**, 12453-12457, doi:10.1002/anie.201806652 (2018).
106 Lieber, C. M. & Lewis, N. S. Catalytic reduction of carbon dioxide at carbon electrodes modified with cobalt phthalocyanine. *Journal of the American Chemical Society* **106**, 5033-5034, doi:10.1021/ja00329a082 (1984).
107 Zhang, X. *et al.* Highly selective and active CO2 reduction electrocatalysts based on cobalt phthalocyanine/carbon nanotube hybrid structures. *Nature Communications* **8**, 14675, doi:10.1038/ncomms14675 (2017).
108 Kramer, W. W. & McCrory, C. C. L. Polymer coordination promotes selective CO2 reduction by cobalt phthalocyanine. *Chemical Science* **7**, 2506-2515, doi:10.1039/C5SC04015A (2016).
109 Liu, Y. & McCrory, C. C. L. Modulating the mechanism of electrocatalytic CO2 reduction by cobalt phthalocyanine through polymer coordination and encapsulation. *Nature Communications* **10**, 1683, doi:10.1038/s41467-019-09626-8 (2019).
110 Diercks, C. S., Liu, Y., Cordova, K. E. & Yaghi, O. M. The role of reticular chemistry in the design of CO2 reduction catalysts. *Nature Materials* **17**, 301-307, doi:10.1038/s41563-018-0033-5 (2018).
111 Jiao, L., Wang, Y., Jiang, H.-L. & Xu, Q. Metal–Organic Frameworks as Platforms for Catalytic Applications. *Advanced Materials* **30**, 1703663, doi:10.1002/adma.201703663 (2018).
112 Matheu, R. *et al.* Three-Dimensional Phthalocyanine Metal-Catecholates for High Electrochemical Carbon Dioxide Reduction. *Journal of the American Chemical Society* **141**, 17081-17085, doi:10.1021/jacs.9b09298 (2019).
113 Lin, S. *et al.* Covalent organic frameworks comprising cobalt porphyrins for catalytic CO_2 reduction in water. *Science* **349**, 1208, doi:10.1126/science.aac8343 (2015).
114 Diercks, C. S. *et al.* Reticular Electronic Tuning of Porphyrin Active Sites in Covalent Organic Frameworks for Electrocatalytic Carbon Dioxide Reduction. *Journal of the American Chemical Society* **140**, 1116-1122, doi:10.1021/jacs.7b11940 (2018).
115 Wu, Q. *et al.* Integration of Strong Electron Transporter Tetrathiafulvalene into Metalloporphyrin-Based Covalent Organic Framework for Highly Efficient Electroreduction of CO2. *ACS Energy Letters* **5**, 1005-1012, doi:10.1021/acsenergylett.9b02756 (2020).
116 Marianov, A. N. & Jiang, Y. Covalent ligation of Co molecular catalyst to carbon cloth for efficient electroreduction of CO2 in water. *Applied Catalysis B: Environmental* **244**, 881-

888, doi:https://doi.org/10.1016/j.apcatb.2018.11.084 (2019).
117 Zhu, M. *et al.* Covalently Grafting Cobalt Porphyrin onto Carbon Nanotubes for Efficient CO2 Electroreduction. *Angewandte Chemie International Edition* **58**, 6595-6599, doi:10.1002/anie.201900499 (2019).
118 Orchanian, N. M., Hong, L. E. & Marinescu, S. C. Immobilized Molecular Wires on Carbon-Cloth Electrodes Facilitate CO2 Electrolysis. *ACS Catalysis* **9**, 9393-9397, doi:10.1021/acscatal.9b03134 (2019).
119 Willkomm, J. *et al.* Grafting of a Molecular Rhenium CO2 Reduction Catalyst onto Colloid-Imprinted Carbon. *ACS Applied Energy Materials* **2**, 2414-2418, doi:10.1021/acsaem.9b00216 (2019).
120 Oh, S., Gallagher, J. R., Miller, J. T. & Surendranath, Y. Graphite-Conjugated Rhenium Catalysts for Carbon Dioxide Reduction. *Journal of the American Chemical Society* **138**, 1820-1823, doi:10.1021/jacs.5b13080 (2016).
121 Jackson, M. N. & Surendranath, Y. Molecular Control of Heterogeneous Electrocatalysis through Graphite Conjugation. *Accounts of Chemical Research* **52**, 3432-3441, doi:10.1021/acs.accounts.9b00439 (2019).
122 Ren, S. *et al.* Molecular electrocatalysts can mediate fast, selective CO_2 reduction in a flow cell. *Science* **365**, 367, doi:10.1126/science.aax4608 (2019).
123 Lu, X. *et al.* High-Performance Electrochemical CO2 Reduction Cells Based on Non-noble Metal Catalysts. *ACS Energy Letters* **3**, 2527-2532, doi:10.1021/acsenergylett.8b01681 (2018).
124 Wang, M. *et al.* CO_2 electrochemical catalytic reduction with a highly active cobalt phthalocyanine. *Nat Commun* **10**, 3602 (2019).
125 Weekes, D. M., Salvatore, D. A., Reyes, A., Huang, A. & Berlinguette, C. P. Electrolytic CO2 Reduction in a Flow Cell. *Accounts of Chemical Research* **51**, 910-918, doi:10.1021/acs.accounts.8b00010 (2018).
126 Jeong, H.-Y. *et al. Achieving highly efficient CO2 to CO electroreduction exceeding 300 mA cm−2 with single-atom nickel electrocatalysts. Journal of Materials Chemistry A* **7**, 10651-10661, doi:10.1039/C9TA02405K (2019).
127 Möller, T. *et al.* Efficient CO2 to CO electrolysis on solid Ni–N–C catalysts at industrial current densities. *Energy & Environmental Science* **12**, 640-647, doi:10.1039/C8EE02662A (2019).
128 Yang, H. *et al.* Carbon dioxide electroreduction on single-atom nickel decorated carbon membranes with industry compatible current densities. *Nature Communications* **11**, 593, doi:10.1038/s41467-020-14402-0 (2020).
129 Lin, L. *et al.* Synergistic Catalysis over Iron-Nitrogen Sites Anchored with Cobalt Phthalocyanine for Efficient CO2 Electroreduction. *Advanced Materials* **31**, 1903470, doi:10.1002/adma.201903470 (2019).
130 Herranz, J., Patru, A., Fabbri, E. & Schmidt, T. J. Co-electrolysis of CO2 and H2O: From electrode reactions to cell-level development. *Current Opinion in Electrochemistry*, doi:https://doi.org/10.1016/j.coelec.2020.05.004 (2020).
131 Ghoshal, S. *et al.* ZIF 67 Based Highly Active Electrocatalysts as Oxygen Electrodes in Water Electrolyzer. *ACS Applied Energy Materials* **2**, 5568-5576, doi:10.1021/acsaem.9b00733 (2019).
132 Li, T. *et al.* Electrolytic Conversion of Bicarbonate into CO in a Flow Cell. *Joule* **3**, 1487-1497, doi:10.1016/j.joule.2019.05.021 (2019).

133 Medina-Ramos, J. *et al.* Cathodic Corrosion at the Bismuth-Ionic Liquid Electrolyte Interface under Conditions for CO_2 Reduction. *Chem. Mater.* **30**, 2362-2373, doi:10.1021/acs.chemmater.8b00050 (2018).

134 Avila-Bolivar, B., Garcia-Cruz, L., Montiel, V. & Solla-Gullon, J. Electrochemical reduction of CO_2 to formate on easily prepared carbon-supported Bi nanoparticles. *Molecules* **24**, 2032pp., doi:10.3390/molecules24112032 (2019).

135 Lv, W., Zhang, R., Gao, P. & Lei, L. Studies on the faradaic efficiency for electrochemical reduction of carbon dioxide to formate on tin electrode. *Journal of Power Sources* **253**, 276-281, doi:10.1016/j.jpowsour.2013.12.063 (2014).

136 Zhai, Y., Gui, F., Guan, S., Sridhar, N. & Agarwal, A. S. Method and Apparatus for the Electrochemical Reduction of Carbon Dioxide, U.S. Patent. 9,145,615 (2015).

137 Zhai, Y., Guan, S., Sridhar, N. & Agarwal, A. S. Electrochemical process. 10253420 (2019).

138 Agarwal, A. S., Rode, E. J. & Gautam, D. Electrochemical Electrode Comprising Tin Basel Catalyst, And Method of Making, US Patent. 10,273,587 (2019).

139 He, S. *et al.* The p-Orbital Delocalization of Main-Group Metals to Boost CO_2 Electroreduction. *Angewandte Chemie International Edition* **57**, 16114-16119, doi:10.1002/anie.201810538 (2018).

140 Garcia de Arquer, F. P. *et al.* 2D Metal Oxyhalide-Derived Catalysts for Efficient CO_2 Electroreduction. *Adv. Mater. (Weinheim, Ger.)* **30**, n/a, doi:10.1002/adma.201802858 (2018).

141 Liu, P. F., Zu, M. Y., Zheng, L. R. & Yang, H. G. Bismuth oxyiodide microflower-derived catalysts for efficient CO_2 electroreduction in a wide negative potential region. *Chem. Commun. (Cambridge, U. K.)* **55**, 12392-12395, doi:10.1039/c9cc05089b (2019).

142 Guo, S.-X. *et al.* Phosphomolybdic Acid-Assisted Growth of Ultrathin Bismuth Nanosheets for Enhanced Electrocatalytic Reduction of CO_2 to Formate. *ChemSusChem* **12**, 1091-1100, doi:10.1002/cssc.201802409 (2019).

143 Li, L., Ma, D.-K., Qi, F., Chen, W. & Huang, S. Bi nanoparticles/Bi2O3 nanosheets with abundant grain boundaries for efficient electrocatalytic CO_2 reduction. *Electrochim. Acta* **298**, 580-586, doi:10.1016/j.electacta.2018.12.116 (2019).

144 Lv, W. *et al.* Bi2O2CO3 Nanosheets as Electrocatalysts for Selective Reduction of CO_2 to Formate at Low Overpotential. *ACS Omega* **2**, 2561-2567, doi:10.1021/acsomega.7b00437 (2017).

145 Meng, F.-L., Zhang, Q., Liu, K.-H. & Zhang, X.-B. Integrated bismuth oxide ultrathin nanosheets/carbon foam electrode for highly selective and energy-efficient electrocatalytic conversion of CO_2 to HCOOH. *Chem. - Eur. J.*, Ahead of Print, doi:10.1002/chem.201903158 (2019).

146 Su, P. *et al.* Ultrathin Bismuth Nanosheets as a Highly Efficient CO_2 Reduction Electrocatalyst. *ChemSusChem* **11**, 848-853, doi:10.1002/cssc.201702229 (2018).

147 Wang, Q., Zhu, C., Wu, C. & Yu, H. Direct synthesis of bismuth nanosheets on a gas diffusion layer as a high-performance cathode for a coupled electrochemical system capable of electroreduction of CO_2 to formate with simultaneous degradation of organic pollutants. *Electrochim. Acta* **319**, 138-147, doi:10.1016/j.electacta.2019.06.167 (2019).

148 Wu, D. *et al.* Electrochemical Transformation of Facet-Controlled BiOI into Mesoporous Bismuth Nanosheets for Selective Electrocatalytic Reduction of CO_2 to Formic Acid. *ChemSusChem* **12**, 4700-4707, doi:10.1002/cssc.201901724 (2019).

149 Yang, H. *et al.* Selective CO_2 Reduction on 2D Mesoporous Bi Nanosheets. *Adv. Energy*

Mater. **8**, n/a, doi:10.1002/aenm.201801536 (2018).
150 Zhang, X., Sun, X., Guo, S.-X., Bond, A. M. & Zhang, J. Formation of lattice-dislocated bismuth nanowires on copper foam for enhanced electrocatalytic CO_2 reduction at low overpotential. *Energy Environ. Sci.* **12**, 1334-1340, doi:10.1039/c9ee00018f (2019).
151 Fan, K. *et al.* Curved Surface Boosts Electrochemical CO_2 Reduction to Formate via Bismuth Nanotubes in a Wide Potential Window. *ACS Catal.* **10**, 358-364, doi:10.1021/acscatal.9b04516 (2020).
152 Kunene, T., Atifi, A. & Rosenthal, J. Selective CO_2 Reduction Over Rose's Metal in the Presence of an Imidazolium Ionic Liquid Electrolyte. *ACS Applied Energy Materials*, doi:10.1021/acsaem.9b01995 (2019).
153 Chu, M. *et al.* Enhancing electroreduction of CO_2 over Bi_2WO_6 nanosheets by oxygen vacancies. *Green Chem.* **21**, 2589-2593, doi:10.1039/c9gc00479c (2019).
154 Daiyan, R. *et al.* Modulating Activity through Defect Engineering of Tin Oxides for Electrochemical CO_2 Reduction. *Adv. Sci. (Weinheim, Ger.)* **6**, 1900678, doi:10.1002/advs.201900678 (2019).
155 Gu, J., Heroguel, F., Luterbacher, J. & Hu, X. Densely Packed, Ultra Small SnO Nanoparticles for Enhanced Activity and Selectivity in Electrochemical CO_2 Reduction. *Angew. Chem., Int. Ed.* **57**, 2943-2947, doi:10.1002/anie.201713003 (2018).
156 Lei, T. *et al.* Continuous electroreduction of carbon dioxide to formate on Tin nanoelectrode using alkaline membrane cell configuration in aqueous medium. *Catalysis Today* **318**, 32-38, doi:10.1016/j.cattod.2017.10.003 (2018).
157 Del Castillo, A., Alvarez-Guerra, M. & Irabien, A. Continuous electroreduction of CO_2 to formate using Sn gas diffusion electrodes. *AIChE Journal* **60**, 3557-3564, doi:10.1002/aic.14544 (2014).
158 Prakash, G. K. S., Viva, F. A. & Olah, G. A. Electrochemical reduction of CO_2 over Sn-Nafion® coated electrode for a fuel-cell-like device. *Journal of Power Sources* **223**, 68-73, doi:10.1016/j.jpowsour.2012.09.036 (2013).
159 Fan, L., Xia, Z., Xu, M., Lu, Y. & Li, Z. 1D SnO2 with Wire-in-Tube Architectures for Highly Selective Electrochemical Reduction of CO_2 to C1 Products. *Adv. Funct. Mater.* **28**, n/a, doi:10.1002/adfm.201706289 (2018).
160 Li, F., Chen, L., Knowles, G. P., MacFarlane, D. R. & Zhang, J. Hierarchical Mesoporous SnO2 Nanosheets on Carbon Cloth: A Robust and Flexible Electrocatalyst for CO_2 Reduction with High Efficiency and Selectivity. *Angewandte Chemie International Edition* **56**, 505-509, doi:10.1002/anie.201608279 (2017).
161 Li, H. *et al.* Promoting the electroreduction of CO_2 with oxygen vacancies on a plasma-activated SnOx/carbon foam monolithic electrode. *Journal of Materials Chemistry A* **8**, 1779-1786, doi:10.1039/C9TA12401B (2020).
162 Zheng, X. *et al.* Theory-guided Sn/Cu alloying for efficient CO_2 electroreduction at low overpotentials. *Nature Catalysis* **2**, 55-61, doi:10.1038/s41929-018-0200-8 (2019).
163 Zhang, J., Yin, R., Shao, Q., Zhu, T. & Huang, X. Oxygen vacancies inaAmorphous InOx nanoribbons enhance CO_2 adsorption and activation for CO_2 electroreduction. *Angew. Chem., Int. Ed.* **58**, 5609-5613, doi:10.1002/anie.201900167 (2019).
164 Hwang, E., Park, H., Kim, H., Ahn, S. H. & Kim, S.-K. Electrochemically Fabricated Pd-In Catalysts for Carbon Dioxide-Formate/Formic Acid Inter-Conversion. *Bull. Korean Chem. Soc.* **38**, 607-613, doi:10.1002/bkcs.11133 (2017).
165 Liu, L. *et al.* Morphology Modulation-Engineered Flowerlike In2S3 via Ionothermal

Method for Efficient CO_2 Electroreduction. *ChemCatChem*, Ahead of Print, doi:10.1002/cctc.201901530 (2019).
166 Xia, Z. *et al.* Highly Selective Electrochemical Conversion of CO_2 to HCOOH on Dendritic Indium Foams. *ChemElectroChem* **5**, 253-259, doi:10.1002/celc.201700935 (2018).
167 Ghosh, S., Garapati, M. S., Ghosh, A. & Sundara, R. Nonprecious Catalyst for Three-Phase Contact in a Proton Exchange Membrane CO_2 Conversion Full Cell for Efficient Electrochemical Reduction of Carbon Dioxide. *ACS Appl. Mater. Interfaces* **11**, 40432-40442, doi:10.1021/acsami.9b11213 (2019).
168 Sekar, P. *et al.* Cobalt Spinel Nanocubes on N-Doped Graphene: A Synergistic Hybrid Electrocatalyst for the Highly Selective Reduction of Carbon Dioxide to Formic Acid. *ACS Catal.* **7**, 7695-7703, doi:10.1021/acscatal.7b02166 (2017).
169 Kang, P., Zhang, S., Meyer, T. J. & Brookhart, M. Rapid Selective Electrocatalytic Reduction of Carbon Dioxide to Formate by an Iridium Pincer Catalyst Immobilized on Carbon Nanotube Electrodes. *Angewandte Chemie International Edition* **53**, 8709-8713, doi:10.1002/anie.201310722 (2014).
170 Chen, L. *et al.* Molecular Catalysis of the Electrochemical and Photochemical Reduction of CO2 with Earth-Abundant Metal Complexes. Selective Production of CO vs HCOOH by Switching of the Metal Center. *Journal of the American Chemical Society* **137**, 10918-10921, doi:10.1021/jacs.5b06535 (2015).
171 Taheri, A., Thompson, E. J., Fettinger, J. C. & Berben, L. A. An Iron Electrocatalyst for Selective Reduction of CO2 to Formate in Water: Including Thermochemical Insights. *ACS Catalysis* **5**, 7140-7151, doi:10.1021/acscatal.5b01708 (2015).
172 Birdja, Y. Y., Shen, J. & Koper, M. T. M. Influence of the metal center of metalloprotoporphyrins on the electrocatalytic CO2 reduction to formic acid. *Catalysis Today* **288**, 37-47, doi:https://doi.org/10.1016/j.cattod.2017.02.046 (2017).
173 Birdja, Y. Y. *et al.* Effects of Substrate and Polymer Encapsulation on CO2 Electroreduction by Immobilized Indium(III) Protoporphyrin. *ACS Catalysis* **8**, 4420-4428, doi:10.1021/acscatal.7b03386 (2018).
174 Wu, J.-X. *et al.* Cathodized copper porphyrin metal–organic framework nanosheets for selective formate and acetate production from CO2 electroreduction. *Chemical Science* **10**, 2199-2205, doi:10.1039/C8SC04344B (2019).
175 Xiaolong Zu, *et al*. Efficient and Robust Carbon Dioxide Electroreduction Enabled by Atomically Dispersed $Sn^{\delta+}$ Sites, Adv. Mater. 31, 1808135. doi:10.1002/adma.201808135 (2019)
176 Gao, J., Ren, D., Guo, X., Zakeeruddin, S. M. & Gratzel, M. Sequential catalysis enables enhanced C-C coupling towards multi-carbon alkenes and alcohols in carbon dioxide reduction: a study on bifunctional Cu/Au electrocatalysts. *Faraday Discuss.* **215**, 282-296, doi:10.1039/c8fd00219c (2019).
177 Morales-Guio, C. G. *et al.* Improved CO_2 reduction activity towards C2+ alcohols on a tandem gold on copper electrocatalyst. *Nat. Catal.* **1**, 764-771, doi:10.1038/s41929-018-0139-9 (2018).
178 Hori, Y., Takahashi, R., Yoshinami, Y. & Murata, A. Electrochemical Reduction of CO at a Copper Electrode. *J. Phys. Chem. B* **101**, 7075, doi:10.1021/jp970284i (1997).
179 Hori, Y., Takahashi, I., Koga, O. & Hoshi, N. Selective Formation of C_2 Compounds from Electrochemical Reduction of CO_2 at a Series of Copper Single Crystal Electrodes. *J. Phys. Chem. B* **106**, 15-17, doi:10.1021/jp013478d (2002).
180 Lee, S. & Lee, J. Ethylene Selectivity in CO Electroreduction when using Cu Oxides: An

In Situ ATR-SEIRAS Study. *ChemElectroChem* **5**, 558-564, doi:10.1002/celc.201700892 (2018).
181 Chen, R. *et al.* Highly Selective Production of Ethylene by the Electroreduction of Carbon Monoxide. *Angew. Chem., Int. Ed.* **59**, 154-160, doi:10.1002/anie.201910662 (2020).
182 Feng, X., Jiang, K., Fan, S. & Kanan, M. W. A Direct Grain-Boundary-Activity Correlation for CO Electroreduction on Cu Nanoparticles. *ACS Central Science* **2**, 169-174, doi:10.1021/acscentsci.6b00022 (2016).
183 Luc, W. *et al.* Two-dimensional copper nanosheets for electrochemical reduction of carbon monoxide to acetate. *Nature Catalysis* **2**, 423-430, doi:10.1038/s41929-019-0269-8 (2019).
184 Gong, M. *et al.* Supramolecular Porphyrin Cages Assembled at Molecular-Materials Interfaces for Electrocatalytic CO Reduction. *ACS Cent. Sci.* **3**, 1032-1040, doi:10.1021/acscentsci.7b00316 (2017).
185 Jouny, M., Luc, W. & Jiao, F. High-rate electroreduction of carbon monoxide to multi-carbon products. *Nat. Catal.* **1**, 748-755, doi:10.1038/s41929-018-0133-2 (2018).
186 Li, J. *et al.* Copper adparticle enabled selective electrosynthesis of n-propanol. *Nat. Commun.* **9**, 1-9, doi:10.1038/s41467-018-07032-0 (2018).
187 Lum, Y. & Ager, J. W. Sequential catalysis controls selectivity in electrochemical CO_2 reduction on Cu. *Energy Environ. Sci.* **11**, 2935-2944, doi:10.1039/c8ee01501e (2018).
188 Wang, X. *et al.* Efficient upgrading of CO to C3 fuel using asymmetric C-C coupling active sites. *Nat. Commun.* **10**, 1-7, doi:10.1038/s41467-019-13190-6 (2019).
189 Wang, L. *et al.* Electrochemically converting carbon monoxide to liquid fuels by directing selectivity with electrode surface area. *Nat. Catal.* **2**, 702-708, doi:10.1038/s41929-019-0301-z (2019).
190 Wang, L. *et al.* Electrochemical Carbon Monoxide Reduction on Polycrystalline Copper: Effects of Potential, Pressure, and pH on Selectivity toward Multicarbon and Oxygenated Products. *ACS Catal.* **8**, 7445-7454, doi:10.1021/acscatal.8b01200 (2018).
191 Bertheussen, E. *et al.* Electroreduction of CO on Polycrystalline Copper at Low Overpotentials. *ACS Energy Lett.* **3**, 634-640, doi:10.1021/acsenergylett.8b00092 (2018).
192 Han, L., Zhou, W. & Xiang, C. High-Rate Electrochemical Reduction of Carbon Monoxide to Ethylene Using Cu-Nanoparticle-Based Gas Diffusion Electrodes. *ACS Energy Letters* **3**, 855-860, doi:10.1021/acsenergylett.8b00164 (2018).
193 Wang, Y., Raciti, D. & Wang, C. High-Flux CO Reduction Enabled by Three-Dimensional Nanostructured Copper Electrodes. *ACS Catal.* **8**, 5657-5663, doi:10.1021/acscatal.8b00902 (2018).
194 Jung, H. *et al.* Electrochemical Fragmentation of Cu_2O Nanoparticles Enhancing Selective C-C Coupling from CO_2 Reduction Reaction. *J. Am. Chem. Soc.* **141**, 4624-4633, doi:10.1021/jacs.8b11237 (2019).
195 Grosse, P. *et al.* Dynamic changes in the structure, chemical state and catalytic selectivity of Cu nanocubes during CO_2 electroreduction: size and support effects. *Angew. Chem., Int. Ed.* **57**, 6192-6197, doi:10.1002/anie.201802083 (2018).
196 Kibria, M. G. *et al.* A Surface Reconstruction Route to High Productivity and Selectivity in CO_2 Electroreduction toward C2+ Hydrocarbons. *Adv. Mater. (Weinheim, Ger.)* **30**, n/a, doi:10.1002/adma.201804867 (2018).
197 Suen, N.-T. *et al.* Morphology Manipulation of Copper Nanocrystals and Product Selectivity in the Electrocatalytic Reduction of Carbon Dioxide. *ACS Catal.* **9**, 5217-5222,

doi:10.1021/acscatal.9b00790 (2019).

198 Fu, J. *et al.* Bipyridine-Assisted Assembly of Au Nanoparticles on Cu Nanowires to Enhance the Electrochemical Reduction of CO_2. *Angew. Chem., Int. Ed.* **58**, 14100-14103, doi:10.1002/anie.201905318 (2019).

199 Wei, X. *et al.* Highly Selective Reduction of CO_2 to C2+ Hydrocarbons at Copper/Polyaniline Interfaces. *ACS Catalysis* **10**, 4103-4111, doi:10.1021/acscatal.0c00049 (2020).

200 Jiao, Y., Zheng, Y., Chen, P., Jaroniec, M. & Qiao, S.-Z. Molecular Scaffolding Strategy with Synergistic Active Centers To Facilitate Electrocatalytic CO_2 Reduction to Hydrocarbon/Alcohol. *J. Am. Chem. Soc.* **139**, 18093-18100, doi:10.1021/jacs.7b10817 (2017).

201 Fan, L. *et al.* Strategies in catalysts and electrolyzer design for electrochemical CO<sub>2</sub> reduction toward C<sub>2+</sub> products. *Science Advances* **6**, eaay3111, doi:10.1126/sciadv.aay3111 (2020).

202 Yano, H., Shirai, F., Nakayama, M. & Ogura, K. Efficient electrochemical conversion of CO_2 to CO, C2H4 and CH4 at a three-phase interface on a Cu net electrode in acidic solution. *Journal of Electroanalytical Chemistry* **519**, 93-100, doi:10.1016/S0022-0728(01)00729-X (2002).

203 Yano, H., Tanaka, T., Nakayama, M. & Ogura, K. Selective electrochemical reduction of CO_2 to ethylene at a three-phase interface on copper(I) halide-confined Cu-mesh electrodes in acidic solutions of potassium halides. *Journal of Electroanalytical Chemistry* **565**, 287-293, doi:10.1016/j.jelechem.2003.10.021 (2004).

204 Kuhl, K. P., Cave, E. R., Abram, D. N. & Jaramillo, T. F. New insights into the electrochemical reduction of carbon dioxide on metallic copper surfaces. *Energy & Environmental Science* **5**, 7050-7059, doi:10.1039/C2EE21234J (2012).

205 Zhao, J. *et al.* An overview of Cu-based heterogeneous electrocatalysts for CO_2 reduction. *Journal of Materials Chemistry A* **8**, 4700-4734, doi:10.1039/C9TA11778D (2020).

206 De Gregorio, G. L. *et al.* Facet-Dependent Selectivity of Cu Catalysts in Electrochemical CO_2 Reduction at Commercially Viable Current Densities. *ACS Catalysis* **10**, 4854-4862, doi:10.1021/acscatal.0c00297 (2020).

207 Masel, R. I. *et al.* in *Commercializing Biobased Products: Opportunities, Challenges, Benefits, and Risks* (ed Seth W. Snyder) 215-257 (Royal Society of Chemistry, 2016).

208 Kim, J. *et al.* Branched Copper Oxide Nanoparticles Induce Highly Selective Ethylene Production by Electrochemical Carbon Dioxide Reduction. *Journal of the American Chemical Society* **141**, 6986-6994, doi:10.1021/jacs.9b00911 (2019).

209 Hoang, T. T. H. *et al.* Nanoporous Copper–Silver Alloys by Additive-Controlled Electrodeposition for the Selective Electroreduction of CO_2 to Ethylene and Ethanol. *Journal of the American Chemical Society* **140**, 5791-5797, doi:10.1021/jacs.8b01868 (2018).

210 Speck, F. D. & Cherevko, S. Electrochemical copper dissolution: A benchmark for stable CO_2 reduction on copper electrocatalysts. *Electrochemistry Communications* **115**, 106739, doi:10.1016/j.elecom.2020.106739 (2020).

211 Dou, S. *et al.* Boosting Electrochemical CO_2 Reduction on Metal-Organic Frameworks via Ligand Doping. *Angew. Chem., Int. Ed.* **58**, 4041-4045, doi:10.1002/anie.201814711 (2019).

212 Masel, R. I. Novel Catalyst Mixtures, U.S. Patent. 8,956,990 (2014).

213 Glueer, A. & Schneider, S. Iron catalyzed hydrogenation and electrochemical reduction of CO_2: The role of functional ligands. *J. Organomet. Chem.* **861**, 159-173, doi:10.1016/j.jorganchem.2018.02.025 (2018).

214 Jiang, X. *et al.* Carbon dioxide electroreduction over imidazolate ligands coordinated with Zn(II) center in ZIFs. *Nano Energy* **52**, 345-350, doi:10.1016/j.nanoen.2018.07.047 (2018).
215 Kim, C. *et al.* Insight into Electrochemical CO_2 Reduction on Surface-Molecule-Mediated Ag Nanoparticles. *ACS Catal.* **7**, 779-785, doi:10.1021/acscatal.6b01862 (2017).
216 Lau, G. P. S. *et al.* New Insights Into the Role of Imidazolium-Based Promoters for the Electroreduction of CO_2 on a Silver Electrode. *J. Am. Chem. Soc.* **138**, 7820-7823, doi:10.1021/jacs.6b03366 (2016).
217 Wang, Z. *et al.* Surface ligand promotion of carbon dioxide reduction through stabilizing chemisorbed reactive intermediates. *J. Phys. Chem. Lett.* **9**, 3057-3061, doi:10.1021/acs.jpclett.8b00959 (2018).
218 Rosen, B. A. *et al.* Ionic Liquid Mediated Selective Conversion of CO_2 to CO At Low Overpotentials. *Science* **334** 643-644, doi:10.1126/science.1209786 (2011).
219 Rosen, B. A., Zhu, W., Kaul, G., Salehi-Khojin, A. & Masel, R. I. Water enhancement of CO_2 conversion on silver in 1-ethyl-3-methylimidazolium tetrafluoroborate. *Journal of the Electrochemical Society* **160**, H138-H141, doi:10.1149/2.004303jes (2013).
220 Zhuang, T.-T. *et al.* Dopant-tuned stabilization of intermediates promotes electrosynthesis of valuable C3 products. *Nat. Commun.* **10**, 1-7, doi:10.1038/s41467-019-12788-0 (2019).
221 Lee, W. H. *et al.* in *Studies in Surface Science and Catalysis* Vol. 68 (eds Calvin H. Bartholomew & John B. Butt) 597-603 (Elsevier, 1991).
222 Gao, D. *et al.* Selective CO_2 Electroreduction to Ethylene and Multicarbon Alcohols via Electrolyte-Driven Nanostructuring. *Angew. Chem., Int. Ed.* **58**, 17047-17053, doi:10.1002/anie.201910155 (2019).
223 Han, Z., Kortlever, R., Chen, H.-Y., Peters, J. C. & Agapie, T. CO_2 Reduction Selective for $C\geq2$ Products on Polycrystalline Copper with N-Substituted Pyridinium Additives A*CS Cent. Sci.* **3**, 853-859, doi:10.1021/acscentsci.7b00180 (2017).
224 McGovern, M. S., Garnett, E. C., Rice, C., Masel, R. I. & Wieckowski, A. Effects of Nafion as a binding agent for unsupported nanoparticle catalysts. *Journal of Power Sources* **115**, 35-39, doi:https://doi.org/10.1016/S0378-7753(02)00623-7 (2003).
225 Zhang, S. *et al.* Polyethylenimine-Enhanced Electrocatalytic Reduction of CO2 to Formate at Nitrogen-Doped Carbon Nanomaterials. *Journal of the American Chemical Society* **136**, 7845-7848, doi:10.1021/ja5031529 (2014).
226 Lau, G. P. S. *et al.* New Insights Into the Role of Imidazolium-Based Promoters for the Electroreduction of CO_2 on a Silver Electrode. *Journal of the American Chemical Society* **138**, 7820-7823, doi:10.1021/jacs.6b03366 (2016).
227 Zhao, S.-F., Horne, M., Bond, A. M. & Zhang, J. Is the Imidazolium Cation a Unique Promoter for Electrocatalytic Reduction of Carbon Dioxide? *The Journal of Physical Chemistry C* **120**, 23989-24001, doi:10.1021/acs.jpcc.6b08182 (2016).

Acknowledgement: Parts of this work were supported by the U.S. Department of Energy, under contracts DE-FE0031706 and DE-SC0018540. The opinions here are those of the authors and may not reflect the opinions of DOE. SR, DC and CB are grateful to the Natural Resources Canada's Energy Innovation Program (RGPIN-2018-06748) and Canadian Institute for Advanced Research (BSE-BERL-162173) for financial support.

Competing Interests: Dioxide Materials is in the business of producing and selling materials for CO_2 electrolyzers including catalyst coated electrodes. RM, ZL, HY, JK, DC have an interest in those sales.

Additional Information Reprints and permission information is available online at www.nature.com/reprints. Correspondence and requests for materials should be addressed to R. Masel.

Figure 1 An artist's illustration of a CO_2 electrode. CO_2 reacts with water and two electrons on the cathode to produce CO and 2 OH^-. The OH^- anions travel through the membrane to the anode. The OH^- anions react on the anode to regenerate the water and electrons, and release oxygen.

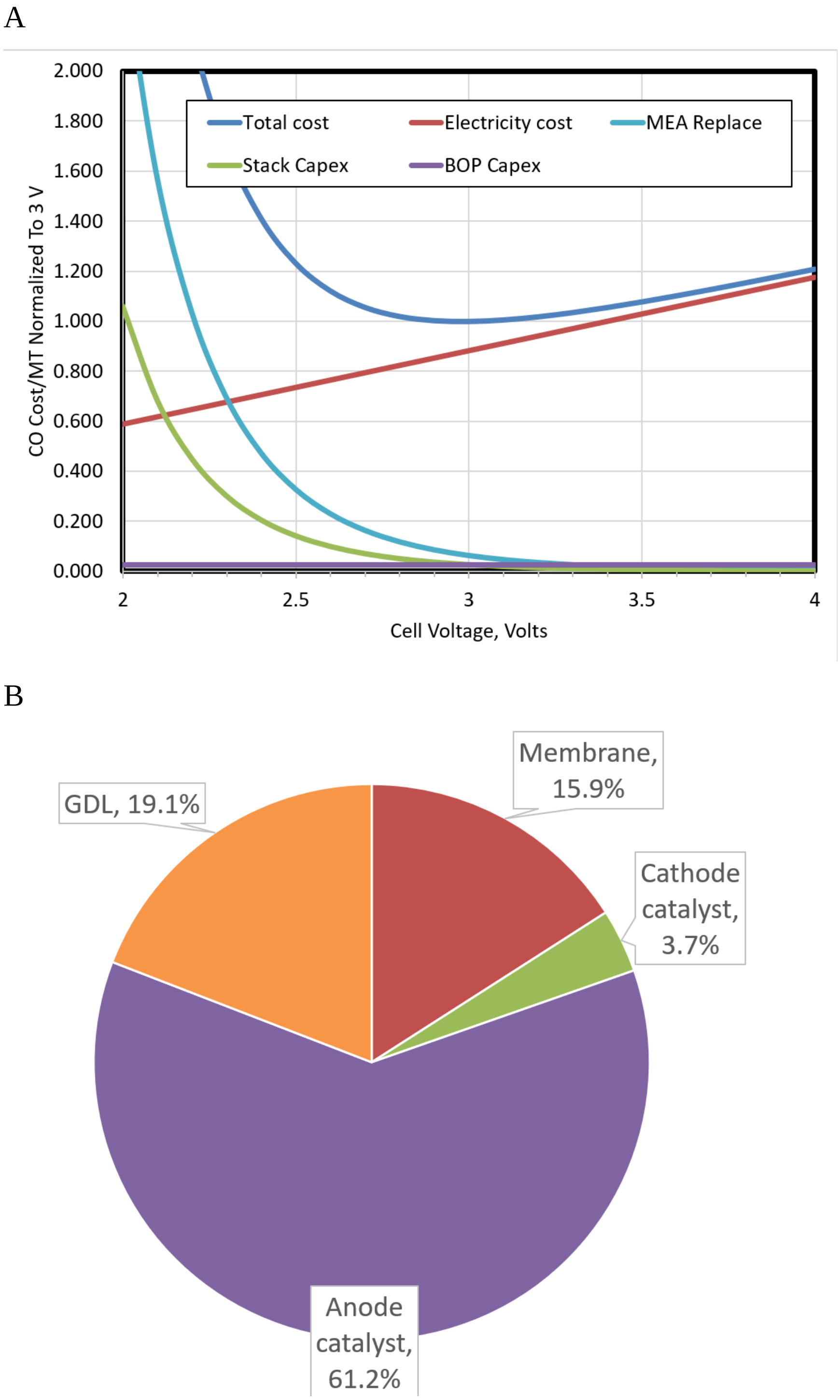

Figure 2. An illustration of how various factors A) The effect of cell voltage on the cost to produce a metric ton (MT) of CO_2 normalized to the cost at 3V. The plot assumes a 5 year membrane electrode assembly (MEA) lifetime, an electricity cost of $0.05/kWh and straight line depreciation of the capital cost over 15 years. The plot also uses actual data for the Sept. 2020 cost of the various components and the voltage/current of Dioxide Materials 5 cm^2 electrolyzers. B) A breakdown of the cost of the MEA using the Sept 2020 cost for the gas diffusion layer (GDL), anode catalyst and cathode catalyst, and Dioxide Materials cost target for the membrane.